BRIEF COMMUNICATION

THE PHOTOCHEMICAL REACTIONS OF BACTERIAL SENSORY RHODOPSIN-I

Flash Photolysis Study in the One Microsecond to Eight Second Time Window

ROBERTO A. BOGOMOLNI* AND JOHN L. SPUDICH‡
*Cardiovascular Research Institute and Department of Biochemistry and Biophysics, University of California, San Francisco, California 94143; and ‡Department of Structural Biology and Department of Physiology and Biophysics, Albert Einstein College of Medicine, Bronx, New York 10461

ABSTRACT *Halobacterium halobium* Flx mutants are deficient in bacteriorhodopsin (bR) and halorhodopsin (hR). Such strains are phototactic and the light signal detectors are two additional retinal pigments, sensory rhodopsins I and II (sR-I and sR-II), which absorb maximally at 587 and 480 nm, respectively. A retinal-deficient Flx mutant, Flx5R, overproduces sR-I-opsin and does not show any photochemical activity other than that of sR-I after the pigment is regenerated by addition of all-*trans* retinal. Using native membrane vesicles from this strain, we have resolved a new photointermediate in the sR-I photocycle between the early bathointermediate S_{610} and the later intermediate S_{373}. The new form, S_{560}, resembles the L intermediate of bR in its position in the photoreaction cycle, its relatively low extinction, and its moderate blue shift. It forms with a half-time of ~90 μs at 21°C, concomitant with the decay of S_{610}. Its decay with a half-time of 270 μs parallels the appearance of S_{373}. From a data set consisting of laser flash-induced absorbance changes (300 ns, 580-nm excitation) measured at 24 wavelengths from 340 to 720 nm in a time window spanning 1 μs to 8 s we have calculated the spectra of the photocycle intermediates assuming a unidirectional, unbranched reaction scheme.

INTRODUCTION

The archaebacterium *Halobacterium halobium* lives in near-saturated brines (for review, see reference 1). Its main energy supply is provided by respiration, but under anaerobic conditions it can use light energy to drive its metabolic functions. The photoenergy transducers are two small (~26 kD), intrinsic membrane chromoproteins, bacteriorhodopsin (bR, λ_{max} 568 nm) and halorhodopsin (hR, λ_{max} 578 nm), which are light-driven electrogenic ion pumps for protons and chloride, respectively (2, 3). The chromophore of each is all-*trans* retinal bound to the ε-amino group of a lysine residue by a protonated Schiff base linkage. Upon photoactivation both bR and hR undergo cyclic photoreactions which are completed in a few milliseconds.

H. halobium cells are polarly flagellated and motile and their swimming behavior is controlled by light stimuli (4–6). Their phototaxis sensitivity is color-discriminating, enabling the cells to migrate into an environment optimal for light energy absorption by bR and hR, while avoiding potentially damaging UV-blue irradiation. Mutants deficient in hR and bR (Flx mutants [7]) are still phototactic and the light signal receptor for the attractant response is an additional retinal-linked chromoprotein, originally named slow-cycling rhodopsin (sR, λ_{max} 587 nm; now sR-I [8, 9]). This photoreceptor, which contains a retinal-linked polypeptide of similar size as bR and hR (10–12), undergoes a cyclic photoreaction that takes seconds to complete and includes a metarhodopsin-like intermediate that absorbs maximally at 373 nm (8). Continuous illumination generates a photostationary state in which S_{373} accumulates. In addition to its slow thermal decay, S_{373} can be reconverted by light to the sR-I_{587} state (8). Under natural light, therefore, the sR-I_{587}/S_{373} system exists in a photochromic photosteady state. On the basis of the sR photoreactions, we proposed a model for color discrimination based on this primitive photochromic system (8). A key element of this proposal is that S_{373} functions as a receptor for repellent phototactic responses to blue and near-UV light, which has been borne out by behavioral studies (13, 14).

A repellent response to wavelengths longer than those absorbed by S_{373} with maximal effect between 450 and 500 nm was detected in some isolates derived from the Flx mutants (15, 16). A second rhodopsin-like pigment (λ_{max}

480 nm) has now been identified spectroscopically (11, 16, 17) and biochemically using retinal radiolabeling (11, 12), and has been referred to as phoborhodopsin (17) or sensory rhodopsin-II (sR-II [11, 12, 16]), with sR renamed sensory rhodopsin-I (sR-I).

Presence of sR-II may have perturbed previous work on sR-I photochemical reactions if the actinic light fell within the sR-II absorption band (8, 24). The retinal-deficient strain Flx5R overproduces the sR-I apoprotein and addition of all-*trans* retinal to Flx5R cells and membranes generates photoactive sR-I and sR-I-mediated phototaxis. Undetectable sR-II is generated according to spectroscopic, retinal radiolabeling and behavioral assays (11, 29; this paper). In the work reported here, the sR-I photoreactions are studied in retinal-regenerated Flx5R membrane vesicles by flash photolysis in the time window spanning 1 μs to 8 s. A new intermediate that can thus be attributed to sR-I has been kinetically resolved and its spectrum and that of all other detected intermediates determined.

MATERIALS AND METHODS

Strains

H. halobium strain Flx5R is a derivative of the bR^-hR^- strain Flx5 (7). Flx5R is blocked in retinal synthesis (ret^-) and was obtained by isolating white (i.e., carotenoid-deficient) colonies, which are often ret^-. Photoreactions of retinal-reconstituted Flx5R membranes indicate relatively abundant sR-I and undetectable sR-II (11).

Sample Preparation

Membrane vesicles were prepared by sonication (18), with final resuspension at 10 mg protein/ml in 4 M NaCl, pH 7.0. The visible absorption spectrum of sR-I, generated by addition of 1 μl of 5 mM all-*trans* retinal in ethanol to 1 ml membrane vesicle suspension, was measured in a double beam spectrophotometer (Lambda 4A; Perkin-Elmer Corp., Norwalk, CT) using unreconstituted Flx5R membranes as a reference. Typically A_{590} obtained was 0.1 for 1-cm pathlength.

Optically clear membrane vesicle pellets were obtained by centrifugation using a Ti80 rotor (Beckman Instruments, Inc., Palo Alto, CA) at 60,000 rpm for 1 h. Wet pellets were withdrawn and mounted between split quartz cuvettes (Hellma Cells, Inc., Jamaica, NY), path length 0.05 cm. Absorbance at 590 nm attributable to sR-I_{587} in the pellets was 0.115.

Data Acquisition

Flash-induced absorbance changes were obtained as described (8), using colinear excitation and measuring beams. Details of the instrument are given by Lozier (19). Maximum kinetic resolution of the instrument was 500 ns/data point. The actinic flash was provided by a flash lamp-pumped dye laser (Phase-R model 1200V; Phase-R Corp., New Durham, NH, 580 nm, 300-ns pulse duration, 0.15 J/flash). Flash repetition rate was 0.12 Hz. The actinic laser was polarized vertically and the measuring beam was polarized at the magic angle with respect to the vertical to avoid contributions of molecular motion to the absorbance transients. Monitoring wavelength half-bandwidth was 4 nm. Temperature was controlled to 21°C ± 1°C using a water-jacketed cuvette holder and circulating water bath.

RESULTS

Flash-induced absorbance changes were obtained in two linear acquisition time windows, 1 μs to 4 ms, and 1 ms to 8 s. This choice of acquisition windows allowed sufficient overlap between traces of the same monitoring wavelength to reliably combine them later into one single trace spanning both time frames for kinetic analysis. Light-induced changes at selected wavelengths are shown in Fig. 1. Absorbance changes at all wavelengths returned to baseline by the end of data collection (8 s). As previously reported (8) we detect a depletion of the pigment's main absorption band and an absorbance increase at wavelengths longer than 600 nm which were not time resolved by our instrument. From the data in Fig. 1 *A* and similar traces at other wavelengths, we determined the difference spectrum at 10 μs after the flash (Fig. 2), which is identical

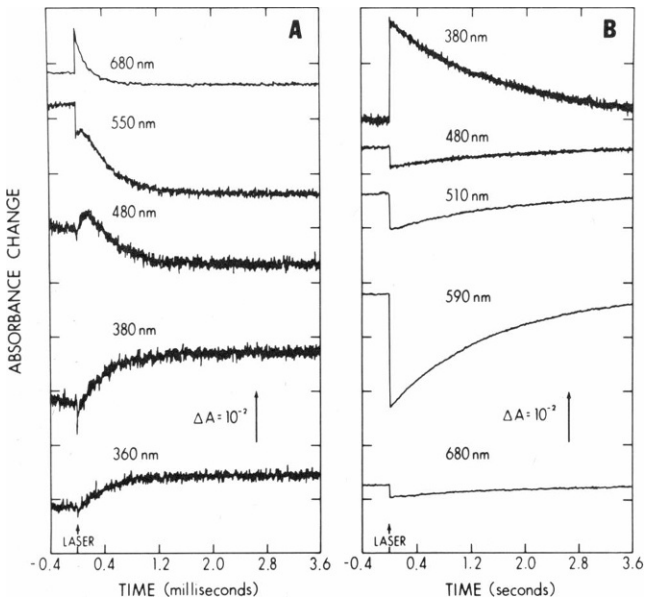

FIGURE 1 Light-induced absorbance changes of sR-I. Monitoring wavelength as indicated on each trace, actinic laser flash (arrow at time 0) and data acquisition as described in Materials and Methods. Traces are average of 16–32 flashes. (*A*) Each trace consists of 4,096 points, 1 μs/point, analogue detector bandwidth 500 ns. The 360 and 380 nm traces plotted at ½ and 480 nm at 2× absorbance increase scale indicated by the vertical arrow. (*B*) Data collected for 8 s, initial 4 s shown. Each trace consists of 4,096 points, 1 ms/point.

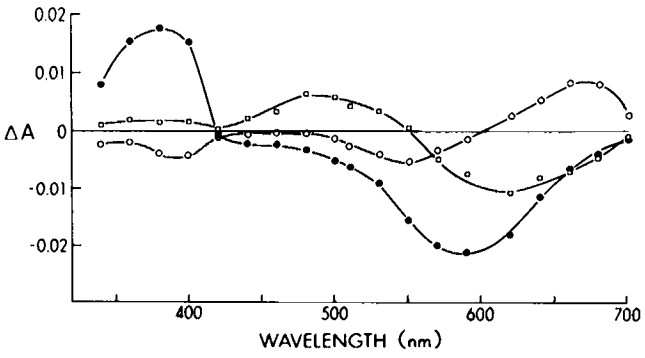

FIGURE 2 Absorption difference spectra. Difference spectra from transient absorbance changes in Fig. 1 as well as additional measurements at other wavelengths. *Open circles*, 0–10 μs. *Open squares*, 10–80 μs. *Solid circles*, 0–3.5 ms.

to the spectrum we obtained in our earlier work and assigned to a red-shifted bathointermediate S_{680}, where the subscript indicates the peak in the difference spectrum (on the basis of its absolute absorption spectrum calculated from the data below, this intermediate will be renamed S_{610} [see below]).

The 10–80-μs time window is characterized by a blue-shift in absorbance. Paralleling S_{610} decay, absorbance is generated at shorter wavelengths, as is especially evident in the 480-nm trace (Fig. 1 *A*), which goes through a maximum and decays in a few hundred microseconds to a long-lived state absorbing farther to the blue. This product of S_{610} decay resembles in its temporal and spectral properties the L intermediate of bR (20). The absorption difference spectrum between 10 and 80 μs (Fig. 2) shows net absorbance increases with a maximum around 480 nm and smaller increases from 340 to 400 nm. The former we attribute to the new L-like intermediate (λ_{max} 510 nm, see below) and the latter to S_{373}. The close correspondence of the 480-nm decay and 380-nm rise (Fig. 1 *A*) suggests a sequential reaction pathway from the L-like intermediate to S_{373}. This long-lived intermediate is characterized by the difference spectrum shown in Fig. 2 (*solid circles*). At long times (1 ms to 3.6 s) the absorbance changes reflect the relaxation of S_{373} to the sR-I_{587} state (Fig. 1 *B*) (8).

Absorbance changes at 24 wavelengths from 340 to 720 nm were well fit by a sum of three exponential components using a standard nonlinear least squares fitting routine (21). Each of the 24 traces yielded consistent values for the three rate constants corresponding to decay half-times t_1 = 80–100 μs, t_2 = 260–290 μs, and t_3 = 730–760 ms, where the ranges represent the minimum and maximum values obtained. The average half-time values (t_1 = 90 μs, t_2 = 270 μs, and t_3 = 750 ms) were used to calculate the absorption spectra of the three photointermediates (Fig. 3) assuming a unidirectional unbranched reaction sequence (Fig. 4) using programs described (22). The fraction of molecules cycling (0.191) was calculated from the absorbance change at 590 nm at 3 ms (ΔA = 0.022).

DISCUSSION

Absolute absorption spectra for early intermediates of the sR-I photochemical cycle have been determined, and a new intermediate has been incorporated in the reaction scheme. A crucial parameter in these calculations is the fraction of molecules cycling. Fortunately the good temporal and spectral separation of the slowest decaying species S_{373} from sR-I_{587} and the earlier intermediates permitted a reliable estimate of this quantity from the absorbance changes at 380 or at 590 nm at 3 ms after flash excitation. Because S_{373} has negligible absorption at 590 nm and all cycling molecules decay into S_{373} by 3 ms, the fraction of photoconverted molecules is simply the fractional depletion of 590 absorbance. A key element in determining the fractional depletion is the knowledge of the absolute absorbance of sR-I_{587} in this complex membrane sample,

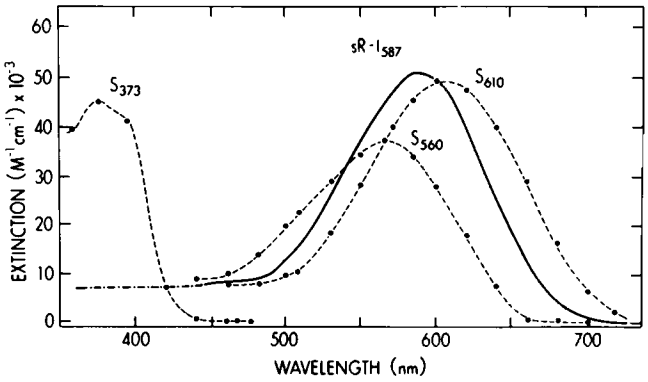

FIGURE 3 Absorption spectra of sR-I photoreaction cycle intermediates. The sR-I_{587} spectrum was determined by retinal regeneration of Flx5R membranes. The spectra of intermediates were obtained using the photocycle scheme and kinetic constants shown in Fig. 4, and the fraction cycling was calculated as described in the text.

which we could readily determine from the absorbance generated by the initial formation of the pigment by retinal addition. Therefore, the only assumption in this estimate of the absorption spectra is that of a linear reaction sequence. Absolute extinction was determined by calculation from the retinal regeneration data.

Data have been presented indicating that below 30°C a branching pathway may occur in membrane preparations with reconversion to sR-I_{587} before S_{373} formation (23, 24). Had a branching pathway occurred in our measurements (21°C), the fraction cycling calculated from the absorbance change at 590 nm would have been underestimated, thereby altering the calculated spectra of all intermediates occurring after the branch. Because in our system we know the absolute absorbance spectrum of sR-I_{587} in the membranes and have obtained the S_{373} absorption spectrum by fully converting sR-I_{587} into S_{373} under continuous intense far red irradiation (13), we have an independent measurement of the fraction cycling from the data in the near-UV. The calculated S_{373} spectrum and the photosteady state

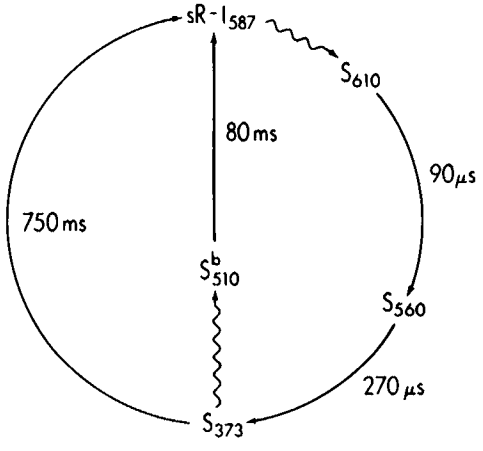

FIGURE 4 Photochemical reaction cycle of sR-I. Wavy arrows indicate light reactions, others indicate thermal reactions for which half-lives are shown. The S_{373} photoreaction path is taken from reference 13.

spectrum (8) are essentially identical in molar extinction and shape, indicating our assumption of a unidirectional unbranched path holds under our experimental conditions.

The 610-nm maximum found for the bathointermediate is at a much shorter wavelength than the peak in the difference spectrum (680 nm), previously used to refer to this species. Because of the quality of the data, the uncertainty in this value, and that of the S_{373} absorption maximum, is <5 nm. The signal to noise for the data in the blue-green range is unfortunately not as high resulting in an estimated uncertainty of ~10 nm in the wavelength maximum of the L-like intermediate.

Previous work comparing the retinal-binding pocket of sR-I and bR using retinal analogue-substituted pigments indicated close similarities in their local electrostatic environments (25). This similarity now extends to their photochemical properties. Close analogies in the spectral and temporal properties of the photointermediates of sR-I and those of bR are evident. S_{610} shows a similar spectral shift and decrease in extinction from sR-I_{587} as K_{590} shows from bR_{568}. This suggests the two pigments undergo similar structural changes in this early step, in which a displacement of the counter ion away from the protonated Schiff base has been invoked (26). Similar spectral changes occur also in later intermediates (compare S_{560} and L_{550}, and S_{373} and M_{412}). From these analogies, we infer that the decay of S_{560} like that of L_{550} of bR leads to deprotonation of the sR-I Schiff base and the resultant large blue-shift. However, S_{373} is closer to the absorption of an unprotonated retinal Schiff base in solution than M_{412}. Interestingly, the visual rhodopsins undergo a reaction sequence more similar to that of sR-I than to that of bR, in that the deprotonated Schiff base form (Metarhodopsin-II in the case of bovine rhodopsin [27, 28]) exhibits an absorption maximum close to that of S_{373}. It is intriguing that these intermediates showing maximum dissociation of retinal/apoprotein interactions have been shown to be signaling states of a number of visual pigments (27, 28) and apparently of sR-I as well (29).

We thank Donald Bivin for providing his nonlinear least squares fitting programs and for his advice.

This work was supported by National Institutes of Health grants GM-27057 (R. A. Bogomolni), GM-34219 (R. A. B.), PCM-8316139 (R. A. B.), and GM-27750 (J. L. Spudich).

Received for publication 15 July 1987 and in final form 8 September 1987.

REFERENCES

1. Stoeckenius W., R. H. Lozier, and R. A. Bogomolni. 1979. Bacteriorhodopsin and the purple membrane of halobacteria. *Biochim. Biophys. Acta.* 505:215–278.
2. Stoeckenius, W., and R. A. Bogomolni. 1982. Bacteriorhodopsin and related pigments of halobacteria. *Annu. Rev. Biochem.* 52:587–615.
3. Lanyi J. K. 1986. Halorhodopsin: a light-driven chloride ion pump. *Annu. Rev. Biophys. Biophys. Chem.* 15:11–28.
4. Spudich, J. L. 1984. Genetic demonstration of a sensory rhodopsin in bacteria. *In* Information and Energy Transduction in Biological Membranes. E. Helmreich, L. Bolis and H. Passow, editors. Alan R. Liss, Inc., New York. 221–229.
5. Hildebrand, E., and A. Schimz. 1985. Behavioral pattern and its photosensory control in *Halobacterium halobium. In* Sensing and Response in Microorganisms. M. Eisenbach and M. Balaban, editors. Elsevier North-Holland, Biomedical Press, Amsterdam. 129–142.
6. Takahashi, T., H. Tomioka, Y. Nakamori, N. Kamo, and Y. Kobatake. 1987. Phototaxis and the second sensory pigment in *Halobacterium halobium. In* The Primary Process in Photobiology. T. Kobayashi, editor. Springer-Verlag New York Inc., NY. In press.
7. Spudich, E. N., and J. L. Spudich. 1982. Control of transmembrane ion fluxes to select halorhodopsin-deficient and other energy transduction mutants of *Halobacterium halobium. Proc. Natl. Acad. Sci. USA.* 79:4308–4312.
8. Bogomolni, R. A., and J. L. Spudich. 1982. Identification of a third rhodopsin-like pigment in phototactic *Halobacterium halobium. Proc. Natl. Acad. Sci. USA.* 79:6250–6254.
9. Spudich, J. L., and R. A. Bogomolni. 1983. Spectroscopic discrimination of the three rhodopsinlike pigments in *Halobacterium halobium* membranes. *Biophys. J.* 43:243–246.
10. Spudich, E. N., R. A. Bogomolni, and J. L. Spudich. 1983. Genetic and biochemical resolution of the chromophoric polypeptide of halorhodopsin. *Biochem. Biophys. Res. Commun.* 112:332–338.
11. Spudich, E. N., S. A. Sundberg, D. Manor, and J. L. Spudich. 1986. Properties of a second sensory receptor protein in *Halobacterium halobium* phototaxis. *Proteins.* 1:239–246.
12. Scherrer P., K. McGinnis, and R. A. Bogomolni. 1987. Biochemical and spectroscopic characterization of the blue-green photoreceptor in *Halobacterium halobium. Proc. Natl. Acad. Sci. USA.* 84:402–406.
13. Spudich, J. L., and R. A. Bogomolni. 1984. Mechanism of colour discrimination by a bacterial sensory rhodopsin. *Nature (Lond.).* 312:509–513.
14. Takahashi, T., Y. Mochizuki, N. Kamo, and Y. Kobatake. 1985. Evidence that the long-lifetime photointermediate of s-rhodopsin is a receptor for negative phototaxis in *Halobacterium halobium. Biochem. Biophys. Res. Commun.* 127:99–105.
15. Takahashi, T., H. Tomioka, N. Kamo, and Y. Kobatake. 1985. A photosystem other than PS370 also mediates the negative phototaxis of *Halobacterium halobium. FEMS (Fed. Eur. Microbiol. Soc.) Microbiol. Lett.* 28:161–164.
16. Wolff, E., R. A. Bogomolni, P. Scherrer, B. Hess, and W. Stoeckenius. 1986. Color discrimination in halobacteria: spectroscopic characterization of a second sensory receptor covering the blue-green region of the spectrum. *Proc. Natl. Acad. Sci. USA.* 83:7272–7276.
17. Tomioka, H., T. Takahashi, N. Kamo, and Y. Kobatake. 1986. Flash spectrophotometric identification of a fourth rhodopsin-like pigment in *Halobacterium halobium. Biochem. Biophys. Res. Commun.* 139:389–395.
18. Lanyi, J. K., and R. E. MacDonald. 1979. Light-induced transport in *Halobacterium halobium. Methods Enzymol.* 56:398–407.
19. Lozier, R. H. 1982. Rapid kinetic optical absorption spectroscopy of bacteriorhodopsin photocycles. *Methods Enzymol.* 88:133–162.
20. Lozier, R. H., R. A. Bogomolni, and W. Stoeckenius. 1975. Bacteriorhodopsin: a light-driven proton pump in *Halobacterium halobium. Biophys. J.* 15:955–962.
21. Helgerson, S. L., M. K. Mathew, D. B. Bivin, P. K. Wolber, E. Heinz, and W. Stoeckenius. 1985. Coupling between the bacteriorhodopsin photocycle and the protonmotive force in *Halobacterium halobium* cell envelope vesicles. III. Time-resolved increase in the transmembrane electric potential and modeling of the associated ion fluxes. *Biophys. J.* 48:709–719.

22. Nagle, J. F., L. A. Parodi, and R. H. Lozier. 1982. Procedure for testing kinetic models of the photocycle of bacteriorhodopsin. *Biophys. J.* 38:161–174.
23. Hazemoto N., N. Kamo, Y. Terayama, Y. Kobatake, and M. Tsuda. 1983. Photochemistry of two rhodopsinlike pigments in bacteriorhodopsin-free mutant of *Halobacterium halobium*. *Biophys. J.* 44:59–64.
24. Ohtami, H., T. Kobayashi, and M. Tsuda. 1986. Photocycle of sensory rhodopsin. A new precursor of sR_{370}. *Photobiochem. Photobiophys.* 13:203–208.
25. Spudich, J. L., D. A. McCain, K. Nakanishi, M. Okabe, N. Shimizu, H. Rodman, B. Honig, and R. A. Bogomolni. 1986. Chromophore/protein interaction in bacterial sensory rhodopsin and bacteriorhodopsin. *Biophys. J.* 49:243–246.
26. Honig, B., T. Ebrey, R. H. Callender, U. Dinur, and M. Ottolenghi. 1979. Photoisomerization, energy storage, and charge separation: a model for light energy transduction in visual pigments and bacteriorhodopsin. *Proc. Natl. Acad. Sci. USA.* 76:2503–2507.
27. Chabre, M. 1985. Trigger and amplification mechanisms in visual transduction. *Annu. Rev. Biophys. Biophys. Chem.* 14:331–360.
28. Stryer, L. 1986. Cyclic GMP cascade of vision. *Annu. Rev. Neurosci.* 9:87–119.
29. McCain, D. A., L. A. Amici, and J. L. Spudich. 1987. Kinetically resolved states of the *Halobacterium halobium* flagellar motor switch and modulation of the switch by sensory rhodopsin I. *J. Bacteriol.* 169:4750–4758.